Catal Lett (2008) 126:333–340
DOI 10.1007/s10562-008-9626-y

# Alkylation of Phenol with tert-Butanol Catalyzed by Mesoporous Material with Enhanced Acidity Synthesized from Zeolite MCM-22

**Ke Song · Jingqi Guan · Shujie Wu · Ying Yang · Bo Liu · Qiubin Kan**

Received: 16 June 2008 / Accepted: 19 August 2008 / Published online: 17 September 2008


**Abstract** Using zeolite MCM-22 as source and cetyltrimethylammonium bromide (CTAB) as template, mesoporous material denoted as M-MCM-22 with enhanced acidity has been synthesized and characterized by XPD, FT-IR, $N_2$ adsorption–desorption, $^{27}$Al-MAS NMR, IR spectra of pyridine adsorption, and $NH_3$-TPD techniques, etc. The catalytic performance of M-MCM-22 was tested in alkylation of phenol with tert-butanol, indicating that M-MCM-22 showed highly and steadily catalytic properties. The highest conversion of phenol could be achieved at 418 K, while the highest selectivity to 2, 4-di-TBP was obtained at 398 K. It is found that high temperature is advantageous to form 4-TBP, whereas low weight hourly space velocity (WHSV/$h^{-1}$) is helpful for both conversion of phenol and selectivity to 2,4-DTBP. It is also shown that high ratio of tert-butanol/phenol is beneficial for obtaining high conversion of phenol and selectivity to 2,4-di-TBP.

**Keywords** Mesoporous · MCM-22 · Enhanced acidity · Butylation · Phenol

## 1 Introduction

Butylation of phenol with tert-butanol is a typical Friedel–Crafts alkylation reaction catalyzed by acid. Catalysts for this reaction include Lewis acids [1] (such as $AlCl_3$ and $BF_3$), Brønsted acids [2] (such as $H_3PO_4$, $H_2SO_4$, HF, $HClO_4$), cation exchange resins [3], metal oxides [4], zeolite [5–9] and mesoporous aluminosilicate materials [10–17], etc. Based on the intensity of acidity, the distribution of products is different. Weak acid catalysts mainly lead to an etherified product such as phenyl ether, *t*-BPE. Moderate acid catalysts give the product of *p*-tert-butyl phenol. If strong acid catalysts are used in the alkylation reaction, 2, 4-di-tert butyl phenol is a dominant product. Based on the kinetics, *o*-tert-butyl phenol is the jarless product of alkylation of phenol with tert-butanol. However, due to steric hindrance, *o*-tert-butyl phenol is isomerized into *p*-tert-butyl phenol readily. Both *p*-tert-butyl phenol and 2, 4-di-tert-butyl phenol are the important feedstock for antioxidants, ultraviolet absorbers and heat stabilizers for polymeric materials in industry [18, 19]. Alkylation of phenol with tert-butanol is an important way to producing the two products. Molecule sieve catalysts have been widely used in the alkylation reaction because of their inherent advantages: uniform pore size, high thermal stability, environmental friendliness, etc [20]. For the alkylation of phenol with tert-butanol over zeolite catalysts, both conversion of phenol and selectivity to products are varied according to different structure and character of zeolites. Among zeolite catalysts, zeolite beta and Y show considerably catalytic properties. However, the pore sizes of these zeolites are too small to form 2, 4-di-TBP and 2, 4, 6-tri-TBP. Although mesoporous materials such as Al-MCM-41, Al-MCM-48, Al-SBA-15 and Al-TUD are used in the alkylation reaction [10–17], the conversion of phenol is lower than that achieved over zeolite beta and zeolite Y, and the selectivity to 2, 4-di-TBP is also low. It is well known that the pore walls of conventional mesoporous materials are amorphous, leading to weak acidity and limitation of use in the alkylation reaction. Therefore, new materials which combine the large pore sizes of mesoporous materials with the strong acidity of microporous zeolites become very attractive.

K. Song · J. Guan · S. Wu · Y. Yang · B. Liu · Q. Kan (✉)
College of Chemistry, Jilin University, Changchun 130023, People's Republic of China
e-mail: qkan@mail.jlu.edu.cn

Up to now, there are several methods to synthesize mesoporous aluminosilicates materials with enhanced acidity: recrystallizing the pore walls of mesostructure; synthesis of microporous and mesoporous composite materials; and synthesis of pure mesophases from preformed zeolite seeds. By recrystallizing the wall of MCM-41 and HMS in the presence of tetrapropylammonium cations, Kloetstra et al. succeeded in improving both the acidity and cracking activity [21]. Using virtue of a mixed template, microporous and mesoporous composites containing MFI zeolite and MCM-41 components were synthesized by Karlsson et al. [22] through two step crystallization process. MCM-41- ZSM-5 composites, MCM-48- ZSM-5 composites and MCM-41- beta composites have been reported by using a dual template method [23–26]. Some mesoporous aluminosilicates materials with high hydrothermal stability and enhanced acidity were also synthesized by using zeolite seeds (zeolite Y, ZSM-5 and beta) as precursors and through two-step crystallization process [27–31].

Here we synthesize a hexagonal mesoporous material denoted as M-MCM-22 with enhanced acidity from zeolite MCM-22 treated with sodium hydroxide solution which is tested for the alkylation of phenol with tert-butanol. The structure and acidity of M-MCM-22 are characterized by several physicochemical methods. Various reaction conditions such as reaction temperature, mole ratios of tert-butanol to phenol and space velocity are studied.

## 2 Experimental

### 2.1 Synthesis

Zeolite MCM-22 was synthesized as follows [32]: 1.244 g Sodium aluminate (41 wt%) was dissolved in a glass vessel with 50 mL distilled water, then 10 mL hexamethyleneimine (HMI) was added with vigorous stirring, and 60 g silicon sol was dropwise added into the foregoing solution. The initial gel composition with molar ratio was: $SiO_2$:0.02 $Al_2O_3$:0.35 HMI:25 $H_2O$. After stirring for 2 h, the gel was aged at 170 °C for 72 h under dynamic condition. The resultant product was then cooled down to room temperature, filtered, washed with distilled water and dried at 100 °C overnight. The as-synthesized sample was calcined at 823 K for 6 h with 1 °C/min of heating rate. The calcined sample was denotes as MCM-22-C.

The mesoporous material was prepared as follows: 1.5 g MCM-22-C was mixed with 30 mL 1 M sodium hydroxide solution, and stirred at 60 °C for 3 h, then 15 mL aqueous solution containing 1.84 g CTAB was added to the foregoing mixture. The pH value of the mixture was adjusted to 8–8.5 using 6 M HCl, and then the mixture was further stirred for 2 h. The final mixture was transferred into a Teflon-lined stainless steel autoclave and aged at 100 °C for 24 h. After cooled down to room temperature, the product was filtrated, washed with distilled water and dried at 100 °C overnight. The as-synthesized sample was calcined in air at 823 K for 6 h with 1 °C/min of heating rate. The final product was denoted as M-MCM-22. Proton forms of M-MCM-22 and zeolite MCM-22 were obtained from ion-exchanging with 1 M $NH_4NO_3$, followed by calcination in flowing air at 773 K for 5 h.

### 2.2 Characterization

Powder X-ray diffraction patterns were recorded on a Shimadzu XRD-6000 diffractometer equipped with Ni-filtered Cu Kα radiation and worked at 40 kV, 30 mA, wavelength $\lambda = 0.15418$ nm at a scanning speed of $1^{\circ}\text{min}^{-1}$ ($2\theta = 1.5$–$10$) and $4\ \text{min}^{-1}$ ($2\theta = 10$–$45$), respectively. $N_2$ adsorption–desorption isotherms at 77 K were recorded with a Micromeritics ASAP 2010 system. Before measurements, the sample was outgassed at 250 °C for 3 h. The specific surface area was calculated by the Brunauer–Emmett–Teller (BET) method. The pore size distributions were calculated by using the Barrett–Joyner–Halenda (BJH) method. The total pore volume was taken at relative pressure of 0.989. $^{27}$Al-MAS NMR spectra were measured on a Varian Unity-400 spectrometer, and the chemical shifts were referred to Al $(H_2O_2)^{3+}$. IR spectra were obtained by using a Nicolet Avatar 370 Dtgs spectroscopy. The IR spectroscopy of pyridine adsorption was performed by using self-supporting pellets which were loaded into an IR cell with $CaF_2$ windows. Before pyridine adsorption, the self-supporting pellet was activated at 473 K for 1 h ($10^{-5}$ Torr). Pyridine was adsorbed for 30 min at room temperature and followed by evacuation at 373 K and 473 K ($10^{-5}$ torr). The infrared spectra were recorded at room temperature. $NH_3$-TPD test was performed as follows: the samples were activated at 500 °C for 1 h in pure argon and then cooled down to 100 °C, followed by adsorption of ammonia for 30 min. The physically adsorbed ammonia was removed in pure argon flow at 100 °C. $NH_3$-TPD measurements were carried out in the range of 100–600 °C at an increasing temperature rate of 10 °C/min.

### 2.3 Tert-butylation of Phenol

Tert-butylation of phenol was carried out in a flow fixed quartz bed reactor. About 0.5 g catalyst was activated at 500 °C in nitrogen for 1 h. After cooled down to reaction temperature, the reaction mixture with different tert-butanol/phenol ratio was injected from the top using a syringe pump. The products were collected and quantified by gas

chromatography (GC-8A, Shimadzu) equipped with XE-60 capillary column after the reaction was on for 2 h.

## 3 Results and Discussion

### 3.1 Characterization of M-MCM-22

#### *3.1.1 XRD Analysis*

The X-ray diffraction patterns of M-MCM-22 are shown in Fig. 1. Both as-synthesized and calcined samples show four distinct diffraction peaks attributed to (100), (110), (200) and (210) in the range of 1.5–10, which are the characteristic peaks of hexagonal *p6mm* symmetry. For the calcined sample, $d_{100}$ spacing is 3.85 nm. In the range of 10–40, only amorphous X-ray patterns are observed. All the X-ray diffraction patterns indicate that M-MCM-22 is characteristic of mesoporous structure.

#### *3.1.2 $N_2$ Adsorption–Desorption Measurement*

Nitrogen adsoption–desorption isotherm and pore size distribution of calcined M-MCM-22 are shown in Fig. 2. Typical IV isotherms with H1 type hysteresis loops are observed. The capillary condensation in the relative pressure range from 0.3 to 0.4 corresponds to framework mesopores and a sharp hysteresis loop in this range indicates that M-MCM-22 has uniform mesoporous channels. A hysteresis loop on the desorption isotherms at about $p/p^0 = 0.45$ suggests the existence of secondary texture mesopores [33]. The pore size distribution of M-MCM-22 centralizes at 2.45 and 3.46 nm for column and texture mesopores, respectively. The BET surface area is very large (approaching to 1,075 $m^2\ g^{-1}$) and the pore volume

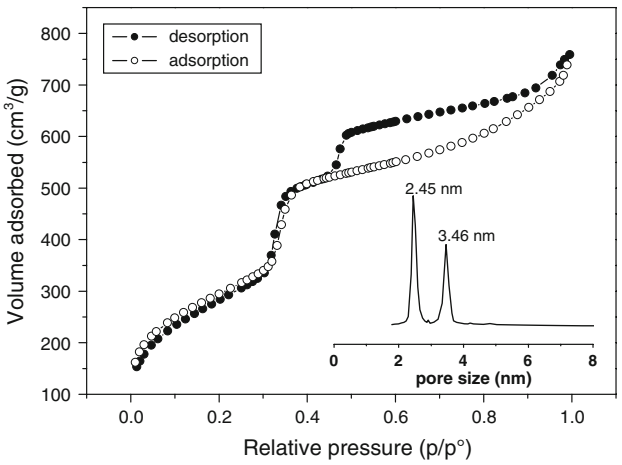


**Fig. 2** $N_2$ Adsorption–desorption isotherms and pore distribution of M-MCM-22

is about 1.0 $cm^3\ g^{-1}$, while the micropores volume of M-MCM-22 is zero as calculated by the *t*-plots method [34], which confirms that M-MCM-22 does not contain micropores.

#### *3.1.3 IR Study*

The IR spectra of Al-MCM-41, MCM-22 and M-MCM-22 are shown in Fig. 3. The bands at 1,217 and 797 $cm^{-1}$ can be assigned to stretching vibrations of Si–O–Si, the band at 1,094 $cm^{-1}$ is attributed to the Si–O stretching vibration, the band at 960 $cm^{-1}$ is derived from the Si–OH vibration at the surface of mesoporous materials, and the bands at 500–600 $cm^{-1}$ come from the five-membered rings of T–O–T (T = Si or Al) in zeolite crystals [35–39]. For zeolite MCM-22, there are three distinct vibration peaks at 500–600 $cm^{-1}$ range, while for Al-MCM-41, vibration peaks at 1217, 1094, 960 and 797 $cm^{-1}$ are distinct, but no

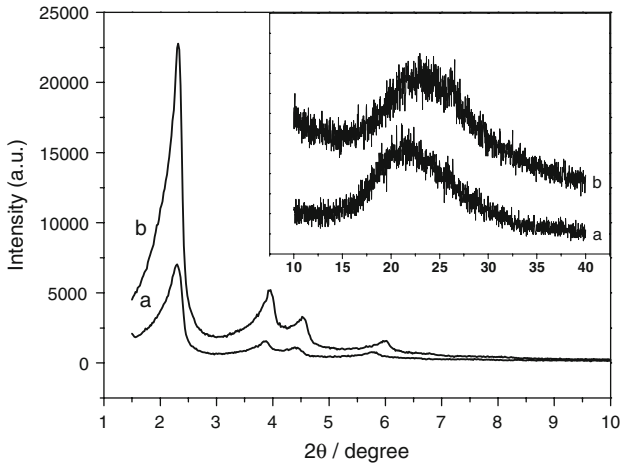


**Fig. 1** XRD patterns of (a) as-synthesized and (b) calcined M-MCM-22

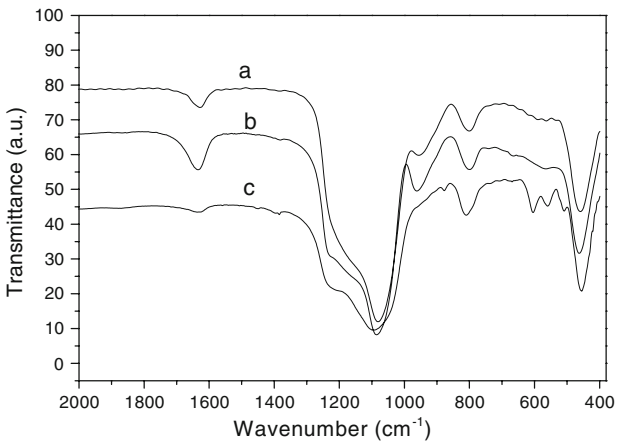


**Fig. 3** IR spectra of (a) calcined M-MCM-22, (b) calcined Al-MCM-41 and (c) calcined zeolite MCM-22

vibration peak is observed in the 500–600 $cm^{-1}$ range due to the amorphous framework. For M-MCM-22, some weak vibration peaks can be seen in the 500–600 $cm^{-1}$ range, which suggests that the framework of M-MCM-22 contain secondary structure of zeolite MCM-22. This characteristic makes M-MCM-22 have tremendous difference from conventional Al-MCM-41, such as acidity. At 960 $cm^{-1}$, the vibration intensity of M-MCM-22 is much less than Al-MCM-41, suggesting that M-MCM-22 have less surface Si–OH than Al-MCM-41.

### *3.1.4 $^{27}$Al-MAS NMR Study*

Figure 4 displays $^{27}$Al-MAS-NMR spectra of the calcined M-MCM-22 and MCM-22. The $^{27}$Al MAS NMR spectra of framework aluminosilicates usually consist of one tetrahedral Al resonance at 54–68 ppm [40]. For calcined M-MCM-22 and MCM-22, the sites of resonance signals are similar centered around 53 ppm, which suggests that Al atoms in M-MCM-22 are completely located in the mesoporous framework.

## 3.2 Acidity of M-MCM-22

### *3.2.1 IR Spectra Analysis of Pyridine Adsorption*

To estimate the type and strength of acid sites of M-MCM-22, IR spectra of pyridine adsorption on M-MCM-22 are studied. As shown in Fig. 5, the bands at 1,454 and 1,624 $cm^{-1}$ are attributed to Lewis acid sites, while the bands at 1,547 and 1,638 $cm^{-1}$ are attributed to Brönsted acid sites. In addition, the band at 1,597 $cm^{-1}$ is attributed to hydrogen-bonded pyridine, whereas, the band at 1,493 $cm^{-1}$ is ascribed to pyridine associated with both Lewis and Brönsted acid sites [41, 42]. Compared with the spectra at 373 K, the intensity of IR peaks only slightly decreases at 573 K, indicating the existence of stronger acid sites of M-MCM-22.

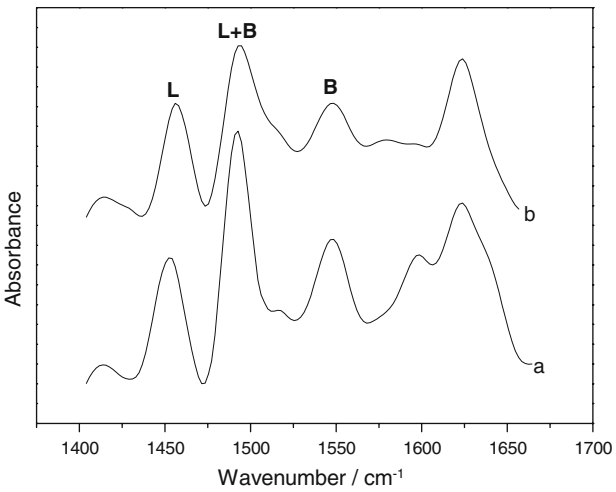


**Fig. 5** IR spectra of pyridine adsorbed on M-MCM-22 at (a) 373 K and (b) 573 K

### *3.2.2 $NH_3$-TPD Study*

The result of $NH_3$-TPD is shown in Fig. 6. For zeolite MCM-22, two peaks at about 480 and 640 K are attributed to weak and strong acid sites, respectively. For M-MCM-22, the broad peak from 170 to 350 °C clearly displays the presence of two different acid sites corresponding to weak and enhanced acid strengths. It means that M-MCM-22 not only has weak acid sites but also has enhanced acid sites, which is different from conventional mesoporous

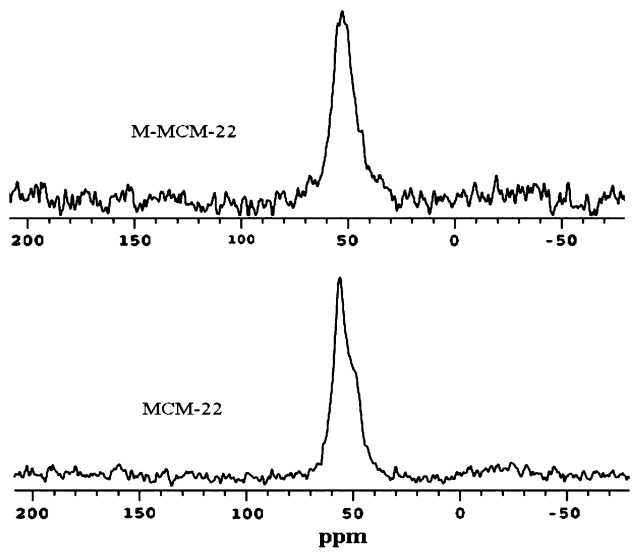


**Fig. 4** $^{27}$Al-MAS NMR spectrum of the calcined M-MMC-22

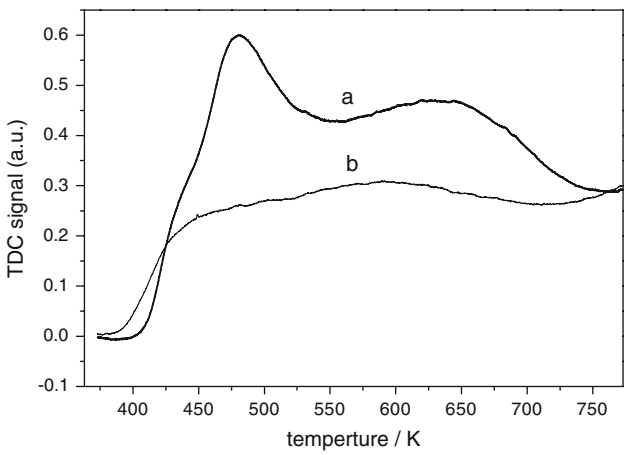


**Fig. 6** $NH_3$-TPD profiles of (a) zeolite MCM-22 and (b) M-MCM-22

aluminosilicate materials containing sole weak acid sites [27–31].

## 3.3 Catalytic Test

### *3.3.1 Comparison of M-MCM-22, MCM-22 and Al-MCM-41*

In order to compare the catalytic activity of M-MCM-22 with Al-MCM-41 and zeolite MCM-22, the catalytic properties of the three samples with similar Si/Al ratio in alkylation reaction of phenol with tert-butanol under the same conditions are studied and the dates are shown in Table 1. Although the pore size of Al-MCM-41 is large enough for the diffusion of the reactants (phenol and tert-butanol) and products (2-TBP, 4-TBP, 2, 4-di-TBP and 2, 4, 6-tri-TBP), both the conversion of phenol (61.3%) and selectivity to 2, 4-di-TBP (13.2%) are low due to the limitation of weak acidity caused by the amorphous pore wall of Al-MCM-41. The pore size of zeolite MCM-22 is larger than the molecular diameters of phenol, tert-butanol and 4-TBP but less than the molecular diameter of 2,4-di-TBP. Therefore, the reactants of phenol and tert-butanol can enter the pore of MCM-22 and the product of 4-TBP can also diffuse out of it, thereby the conversion of phenol is very high (94.0%) and the selectivity to 4-TBP is approaching to 67.0% over MCM-22. However, the pore size of MCM-22 is not advantageous to the product 2,4-di-TBP, and the selectivity to 2, 4-di-TBP (30.6%) is relatively low. On the other hand, M-MCM-22 not only has large enough mesopores but also possesses enhanced acid sites compared with Al-MCM-41, therefore, the conversion of phenol and selectivity to 2,4-di-TBP are as high as 93.3 and 53.9%, respectively. In addition, 2, 4, 6-tri-TBP is also detected.

### *3.3.2 Effect of Reaction Conditions on Alkylation of Phenol with Tert-butanol over M-MCM-22*

The results of phenol conversion over M-MCM-22 at different reaction temperatures and times are displayed in Fig. 7. At a low reaction temperature (378 K), the conversion of phenol is initially high, while it decreases as the reaction time increases. It is caused by pore jam of

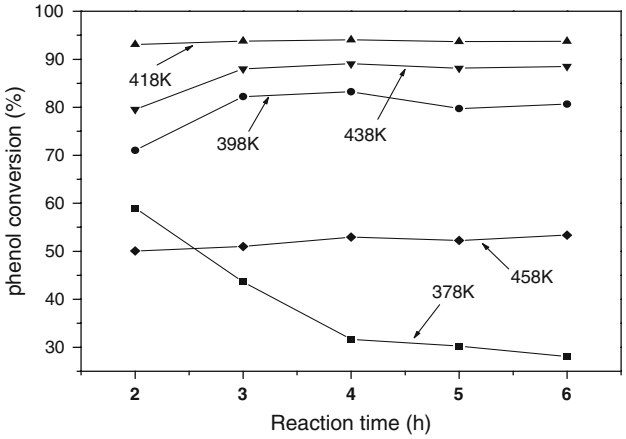


**Fig. 7** Effect of reaction temperature and time on phenol conversion over M-MCM-22 with TBP/phenol = 2.5 and WHSV = 2.2 $h^{-1}$

M-MCM-22. At the primal time, the pore of M-MCM-22 is expedite and the reactants and products can diffuse in the pore channel easily. However, with increasing reaction time, the pore of M-MCM-22 is jammed by the products at low temperature, leading to the reduction of conversion of phenol and selectivity to 2, 4-di-TBP. As the reaction temperature is increased, the conversion of phenol gradually increases. The conversion of phenol approaches to a maximum of 94% when the reaction temperature is 418 K. Further increasing reaction temperature results in a decrease of conversion of phenol. At 458 K, the conversion of phenol is only 52%. It is noted that the selectivity to 2, 4-di-TBP reaches the highest (53%) at 398 K as shown in Fig. 8, and then it decreases with increasing temperature owing to the dealkylation of products at high temperature [10–17]. The selectivity to 4-TBP increases with increasing temperature all through, while the selectivity to 2-TBP shows a contrary trend. A moderate reaction temperature is helpful to produce 2, 4-di-TBP, while a high reaction temperature promotes the isomerization of 2-TBP to 4-TBP. At reaction temperature between 398 and 458 K, M-MCM-22 displays stably catalytic activity and selectivity for alkylation of phenol with tert-butanol.

The influence of space velocity on activity and selectivity of M-MCM-22 is studied at 418 K with tert-butanol/phenol ratio of 3:1 and the results are listed in Table 2.

**Table 1** Catalytic activity and product distribution

Catalysts weight = 0.5 g; Reaction temperature = 418K; $n_{\text{tert-butanol}}/n_{\text{phenol}}$ = 2.5; WHSV = 2.2 $h^{-1}$; time-on-stream = 2 h

| Catalysts | Phenol conversion (mol%) | Products selectivity (mol%) | | | |
|---|---|---|---|---|---|
| | | 2-TBP | 4-TBP | 2,4-DTBP | 2,4,6-TTBP |
| Al-MCM-41 | 61.3 | 4.9 | 81.9 | 13.2 | – |
| MCM-22 | 94.0 | 2.4 | 67.0 | 30.6 | – |
| M-MCM-22 | 93.3 | 3.2 | 41.0 | 53.9 | 1.9 |

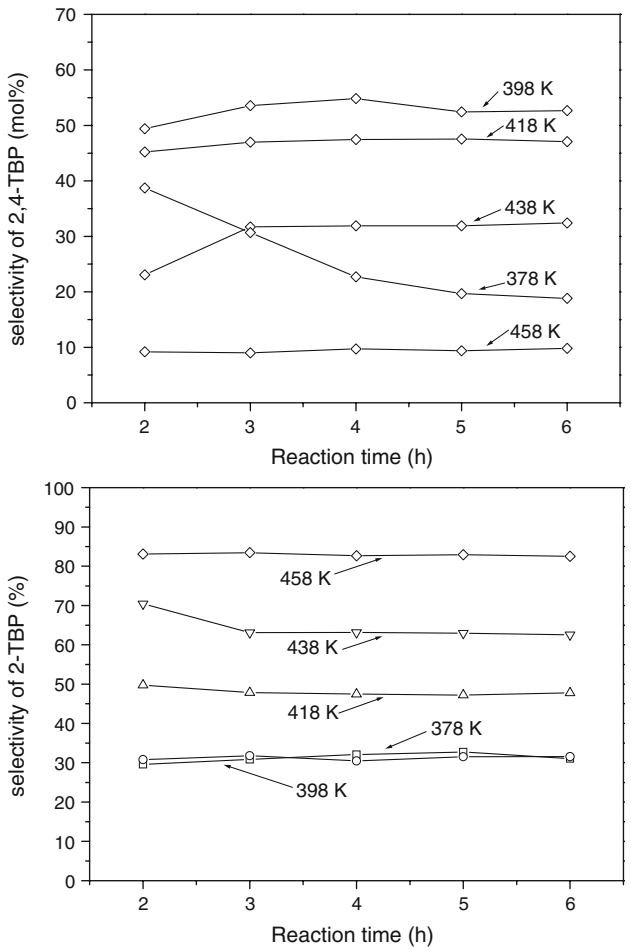


**Fig. 8** Effect of reaction temperature and time on selectivities of 2, 4-di-TBP and 4-TBP over M-MCM-22 with TBP/phenol = 2.5 and WHSV = 2.2 $h^{-1}$

According to a previous report [10–17], in the alkylation reactions of phenol with tert-butanol, tert-butanol is first dehydrated to isobutene and then isobutene reacts with phenol to produce 2-TBP, 4-TBP, 2,4-di-TBP and 2,4,6-tri-TBP over acid sites as indicated in Fig. 9. When the WHSV is reduced, the contact time of both tert-butanol and phenol with acid centers increases, which favors both isobutene formation and reactions with phenol, especially beneficial to generate of more substituted phenol. For example, the phenol conversion increases from 72.3% to 96.3% when the WHSV is reduced from 6.5 to 2.2 $h^{-1}$. At the same time, the selectivity to 2-TBP decreases, whereas the selectivities to 2, 4-di-TBP and 2,4,6-tri-TBP increase with decreasing WHSV because 2-TBP and 4-TBP can further be transformed into 2, 4-di-TBP and 2,4,6-tri-TBP at a long contact time over enhanced acid sites.

Figure 10 displays the effect of tert-butanol/phenol molar ratio on alkylation of phenol with tert-butanol. It is clear that increasing tert-butanol/phenol ratio can raise the conversion of phenol and the selectivity to 2,4-di-TBP, but reduce the selectivities to both 2-TBP and 4-TBP. It is comprehensible that more tert-butanol gives rise to the formation of more isobutene by dehydration and the transformation of more phenol. At the same time, the 2-TBP and 4-TBP are easily transformed into 2,4-di-TBP in the case of more isobutene.

## 4 Conclusion

Templated by CTAB, mesoporous aluminosilicate M-MCM-22 was synthesized from zeolite MCM-22 and characterized by XRD, $N_2$ adsorption–desorption, $^{27}$Al-MAS NMR, pyridine adsorbed FT-IR spectroscopy and $NH_3$-TPD techniques. Analytic results show that M-MCM-22 has ordered hexagonal *p6mm* mesostructure and its framework contains the secondary structure of zeolite MCM-22, which makes the acidity of M-MCM-22 stronger in comparison with conventional Al-MCM-41. $^{27}$Al MAS NMR study confirms that aluminum in M-MCM-22 is exclusively in tetrahedral coordination. In alkylation reactions of phenol with tert-butanol, M-MCM-22 displays higher phenol conversion and 2,4-di-TBP selectivity than conventional mesoporous Al-MCM-41, and also higher 2,4-di-TBP selectivity than microporous MCM-22. In the temperature range from 398 to 438 K, high temperature is beneficial to 4-TBP, while low temperature is helpful to 2-TBP. Moreover, moderate reaction temperature is advantageous to 2,4-di-TBP. Both low space velocity and high molar ratio of tert-butanol/phenol are beneficial to the conversion of phenol and selectivity to 2,4-di-TBP. In addition, M-MCM-22 displays considerable stability in alkylation of phenol with tert-butanol.

**Table 2** Effect of WHSV ($h^{-1}$) on alkylation of phenol with tert-butanol over M-MCM-22

Catalysts weight = 0.5 g; Reaction temperature = 418K; $n_{\text{tert-butanol}}/n_{\text{phenol}}$ = 2.5; Time-on-stream = 2 h

| WHSV/$h^{-1}$ | Phenol conversion (%) | Selectivity of products (mol%) | | | |
|---|---|---|---|---|---|
| | | 2,4,6-tri-TBP | 2-TBP | 4-TBP | 2,4-di-TBP |
| 2.2 | 96.29 | 2.27 | 2.80 | 38.63 | 56.16 |
| 3.0 | 92.53 | 1.42 | 4.0 | 47.50 | 46.95 |
| 6.5 | 72.33 | 0.55 | 11.86 | 55.82 | 32.97 |

**Fig. 9** Process of alkylation of phenol with tert-butanol

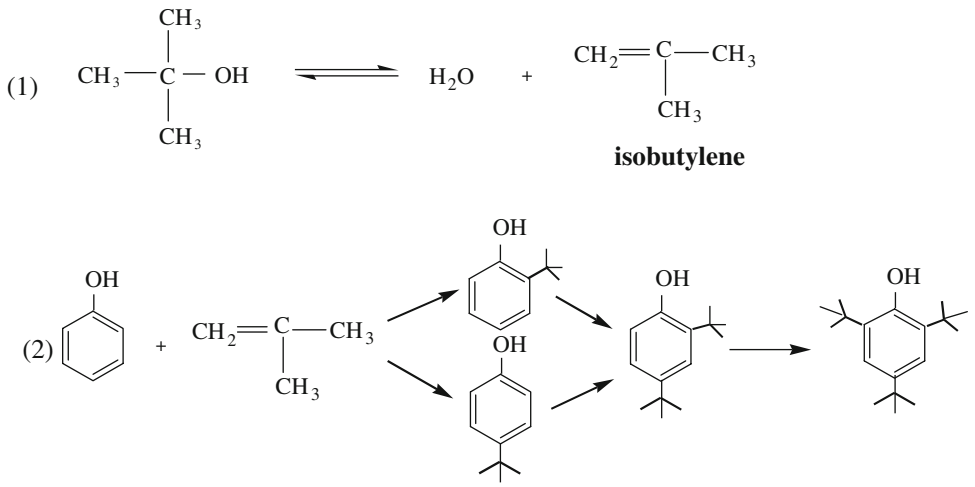


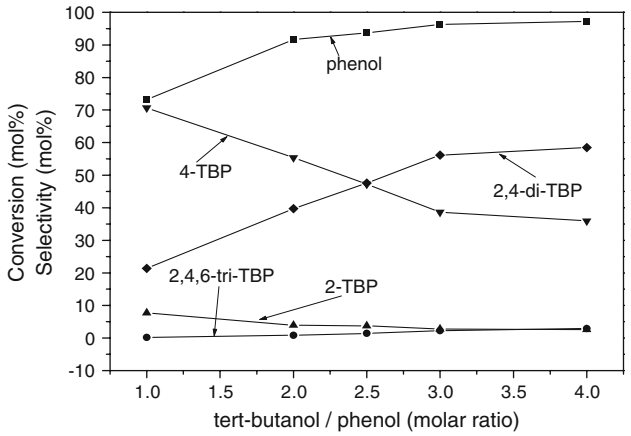


**Fig. 10** Effect of tert-butanol/phenol molar ratio on phenol conversion and product selectivity over M-MCM-22 at 418 K with WHSV = 2.2 $h^{-1}$

**Acknowledgments** We thank the National Basic Research Program of China (2004CB217804) and the National Natural Science Foundation of China (20673046) for financial support of this work.

## References

1. Sartori G, Bigi F, Casiraghi G, Carnati G, Chiesi L, Arduini A (1985) Chem Ind 22:762–763
2. Carlton AA (1948) J Org Chem 13:120
3. Chandra KG, Sharma MM (1993) Catal Lett 19:309–317
4. Sartori G, Bigi F, Casiraghi G, Casnati G, Chiesi L, Arduini A (1985) Chem Ind (London) 22:762–763
5. Krishnan AV, Ojha K, Pradhan NC (2002) Org Process Res Dev 6:132–137
6. Zhang K, Zhang H, Xua G, Xiang S, Xu D, Liu S, Li H (2001) Appl Catal A: Gen 207:183–190
7. Zhang K, Huang C, Zhang H, Xiang S, Liu S, Xu D, Li H (1998) Appl Catal A: Gen 166:89–95
8. Anand R, Maheswari R, Gore KU, Tope BB (2003) J Mol Catal A 193:251–257
9. Dumitriu E, Hulea V (2003) J Catal 218:249–257
10. Vinu A, Devassy BM, Halligudi SB, Bohlmann W, Hartmann M (2005) Appl Catal A: Gen 281:207–213
11. Dapurkar SE, Selvam P (2003) Appl Catal A: Gen 254:239–249
12. Yadav GD, Pathre GS (2006) Appl Catal A: Gen 297:237–246
13. Sakthivel A, Badamali SK, Selvam P (2000) Micropor Mesopor Mater 39:457–463
14. Anand R, Maheswari R, Hanefeld U (2006) J Catal 242:82–91
15. Huang J, Li G, Wu S, Wang H, Xing L, Song K, Wu T, Kan Q (2005) J Mater Chem 15:1055–1060
16. Huang J, Li G, Wu S, Wang H, Xing L, Song K, Wu T, Kan Q (2006) Micropor Mesopor Mater 96:21–28
17. Huang J, Li G, Wu S, Wang H, Xing L, Song K, Wu T, Kan Q (2006) J Catal 242:82–91
18. Knop A, Pilato LA (1985) Phenolic resin chemistry Springer, Berlin
19. Kolka AJ, Napolitano JP, Elike GG (1956) J Org Chem 21:712–713
20. Corma A (1997) Chem Rev 97:2373–2419
21. Kloetstra KR, van Bekkum H, Jansen JC (1997) Chem Commun 2281–2282
22. Karlsson A, Stocker M, Schmidt R (1999) Micropor Mesopor Mater 27:181–192
23. Huang L, Guo W, Deng P, Xue Z, Li Q (2000) J. Phys Chem B 104:2817–2823
24. Xia Y, Mokaya R (2004) J Mater Chem 14:863–870
25. Guo W, Xiong C, Huang L, Li Q (2001) J Mater Chem 11:1886–1890
26. Guo W, Huang L, Deng P, Xue Z, Li Q (2001) Micropor Mesopor Mater 44:427–434
27. Liu Y, Zhang W, Pinnavaia TJ (2000) J Am Chem Soc 122:8791
28. Liu Y, Zhang W, Pinnavaia TJ (2001) Angew Chem In Ed 40:1255–1258
29. Liu Y, Pinnavaia J (2002) Chem Mater 14:3–5
30. Zhang ZT, Han Y, Zhu L, Wang R, Yu Y, Qiu S, Zhao D, Xiao F (2001) Angew Chem Int Ed 40:1258–1262
31. Zhang ZT, Han Y, Xiao F, Qiu S, Zhu L, Wang R, Yu Y, Zhang Z, Zou B, Wang Y, Sun H, Zhao D, Wei Y (2001) J Am Chem Soc 123:5014–5021
32. Wu P, Kan Q, Wang D, Xing H, Jia M, Wu T (2005) Catal Commun 6:449–453
33. Ordomsky VV, Murzin VY, Monakhova YV, Zubavichus YV, Knyazeva EE, Nesterenko NS, Ivanova II (2007) Micropor Mesopor Mater 105:101–110
34. Lippens BC, De Boer JH (1965) J Catal 4:319–323
35. Liu Y, Zhang W, Pinnavaia TJ (2001) Angew Chem Int Ed 40:1255–1258

36. Jacobs PA, Derouane EG, Weitkamp J (1981) J Chem Soc Chem Commun 591–593
37. Jansen JC, Gaag FJV, Bekkum HV (1984) Zeolites 4:369
38. Schoeman BJ (1997) Stud Surf Sci Catal 105:647–654
39. Kirschhock CEA, Ravishankar R, Verspeurt F, Grobet PJ, Jacobs PA, Martens JA (1999) J Phys Chem B 103:4965–4971
40. Lawton SL, Fung AS, Kennedy GJ, Alemany LB, Chang CD, Hatzikos GH, Lissy DN, Rubin MK, Timken H-KC, Steuernagel S, Woessner DE (1996) J Phys Chem 100:3788–3798
41. Parry EP (1963) J Catal 2:371
42. Yamamoto T, Tanaka T, Funabiki T, Yoshida S (1998) J Phys Chem B 102:5830–5839